

# Masked Vision and Language Modeling for Multi-modal Representation Learning

Gukyeong Kwon, Zhaowei Cai, Avinash Ravichandran  
Erhan Bas, Rahul Bhotika, Stefano Soatto

AWS AI Labs

{gukyeong,zhaoweic,ravinash,erhanbas,bhotikar,soattos}@amazon.com

## Abstract

In this paper, we study how to use masked signal modeling in vision and language (V+L) representation learning. Instead of developing masked language modeling (MLM) and masked image modeling (MIM) independently, we propose to build joint masked vision and language modeling, where the masked signal of one modality is reconstructed with the help from another modality. This is motivated by the nature of image-text paired data that both of the image and the text convey almost the same information but in different formats. The masked signal reconstruction of one modality conditioned on another modality can also implicitly learn cross-modal alignment between language tokens and image patches. Our experiments on various V+L tasks show that the proposed method not only achieves state-of-the-art performances by using a large amount of data, but also outperforms the other competitors by a significant margin in the regimes of limited training data.

## 1 Introduction

Vision and language (V+L) representation learning has gained significant attention due to the transferability of the representations for diverse downstream tasks such as zero- or few-shot visual recognition [19, 37, 48], object detection [4, 20], information retrieval [25, 26], and multi-modal generation [40, 41] etc. This success is mainly driven by large-scale pre-training with paired image and text data. V+L pre-training techniques particularly focuses on learning the representations that characterize the association between V+L and are largely been inspired by self-supervised learning techniques [10, 18] in uni-modal learning.

Masked signal modeling is a popular self-supervisory pre-training task [10, 30, 54, 2, 52, 17], which aims at reconstructing the masked signals from the unmasked ones. It has been independently explored in the domains of natural language processing (NLP) and computer vision [10, 30, 54, 2, 52, 17]. For example, in the domain of NLP, BERT [10] and several follow-up works [30, 54] utilize masked language modeling (MLM) where the model is expected to predict the masked text tokens using unmasked tokens. They have shown that MLM leads to powerful generalization performance across diverse NLP tasks. In the domain of computer vision, as shown in the top-left of Figure 1, the masked image modeling (MIM) is to predict masked pixels or image patches using unmasked portions of the images. MIM has shown to be an effective pre-training task for learning visual representations [2, 52, 17].

While MLM and MIM have been actively explored in each domain, existing works do not fully utilize the masked multi-modal signals modeling in the domain of V+L. For example, as shown in the bottom-left of Figure 1, several approaches rely only on MLM with unmasked images and do not model the masked images [13, 25, 26, 27, 53]. In this case, the distribution of text given image,  $p(T|I)$ , can be learned but the distribution of image given text,  $P(I|T)$ , cannot be learned. We show that this potentially leads to biased performance in information retrieval tasks such as image-based

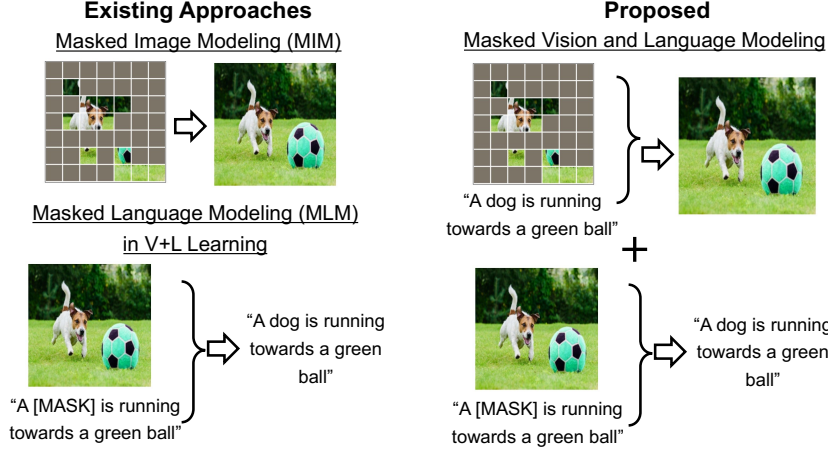


Figure 1: An overview of masked vision and language modeling.

caption retrieval or caption-based image retrieval. Although there exist works that use both modality signals masked, region-based image features extracted from a frozen object detector are masked instead of raw RGB pixels [6, 24, 32, 45, 47]. In this case, the model learns the interactions between extracted image features and texts. The interactions are limited by the extracted image features and the frozen object detector can be a bottleneck to achieve the transferability of V+L representations.

In this paper, we study joint masked V+L modeling where the original signal is reconstructed by using its masked input and the corresponding unmasked input from the other modality. As illustrated in the right-hand side example of Figure 1, the face of the dog in the image can be used to predict the masked text token “dog” and the text “green ball” can be used to reconstruct the corresponding patches in the image. To ensure that the model uses information from both modalities, we explicitly enforce the model to utilize attentions obtained from the other modality signals (cross-attention) to generate the joint representations. Compared to aforementioned existing works, our approach models both conditional distributions,  $p(I|T)$  and  $p(T|I)$ . Also, the model is trained end-to-end and there is no frozen bottleneck model that disturbs learning interactions between V+L. By reconstructing one modality signal from the corresponding the other modality signal (e.g. text “dog” from the face of “dog” in the image), the model implicitly learns the alignment between V+L. Overall, our contributions are summarized as the following:

1. We propose a joint masked vision and language modeling task for V+L representation learning. We show that models pre-trained with the proposed task achieves state-of-the-art performance on a broad range of V+L tasks.
2. We provide a probabilistic interpretation of the proposed method and highlight the difference between ours and existing approaches in terms of the V+L joint distribution estimation.
3. We achieve significantly better performance than other V+L models in the regimes of limited training data and only  $\sim 40\%$  of data used by the compared models is sufficient to match their performance.

## 2 Related work

### 2.1 Vision and language representation learning

The methods in V+L representation learning can be categorized based on how the information is fused between the modalities to obtain the joint representations. We group the fusion techniques into three categories: 1) transformers with attention across modalities, 2) contrastive learning with a large-scale pre-training data, 3) a hybrid form of learning with cross-attention and a contrastive loss. The attention across modalities has been widely used with image features extracted from off-the-shelf object detectors and text features obtained from transformer encoders [6, 24, 32, 47, 55, 28, 45, 27]. While cross-attention effectively aligns V+L representations, it is computationally expensive since all possible pairs of images and texts need to be processed. On the contrary, the authors in [19, 37,

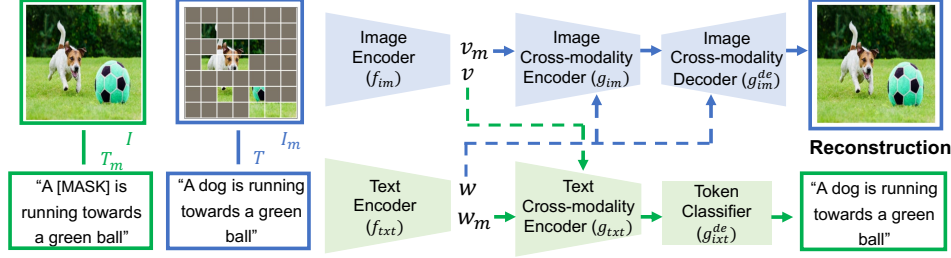


Figure 2: A framework of joint modeling of masked vision and language. The blue and green lines demonstrate the information flow for image and text reconstruction, respectively. The dotted line indicate the cross-modal input for generating attention. The unmasked signals are used as keys and values for the cross-attention layers.

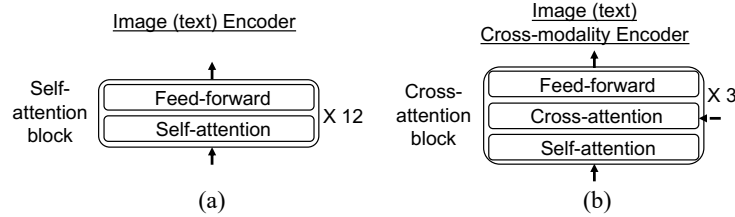


Figure 3: Visualization of image (text) encoders and image (text) cross-modality encoders.

[33, 43] show that contrastive learning with uni-modal encoders and millions of image-text pairs can achieve powerful zero-shot performance in diverse V+L tasks. The contrastive learning-based approaches do not rely on computationally expensive cross-attention but require an excessively large amount of training data. Hence, a combination of contrastive loss and cross-attention is utilized by complementing limitations of both approaches in [26, 25, 53, 13]. In particular, only image and text pairs that result in high similarity by uni-modal encoders are processed using the cross-attention layers to reduce the computational burden and improve the alignment.

## 2.2 Masked Signal Modeling

One of the pre-training objectives that the aforementioned V+L models commonly exploit is masked signal modeling. Masked signal modeling has been independently explored in each of V+L domains. In the NLP domain, BERT and its variants [10, 30] achieve representations that can generalize to a broad range of NLP tasks through MLM. Autoregressive language models [38, 39] which predict masked future tokens have shown to be effective self-supervised learners. The success of the language models leads to several MIM techniques. BeiT [2] is trained to recover masked visual tokens which are obtained by a discrete variational autoencoder (dVAE). In SimMIM [52] and MAE [17], transformers are trained to recover masked patches in an end-to-end fashion. The authors in [5] propose to autoregressively predict the unknown pixels to learn visual representations. In the domain of V+L learning, there exist limited works on end-to-end joint modeling of V+L signals. V+L models with an object detector often aim at recovering only bounding box image features. [6, 24, 32, 47, 45]. In [12, 14], image tokens defined by the dVAE are recovered rather than the raw RGB pixels. The authors in [1] explore MIM and MLM for catalog data with short text attributes. In our work, we train a model to jointly recover V+L signals from masked image patches and masked text tokens. We do not rely on image tokenizers such as dVAE and directly reconstruct RGB pixels. Therefore, MIM and MLM are seamlessly combined to achieve generalizable V+L representations with a simple training framework.

## 3 Method

Our pre-training methods have two types of training objectives, which are 1) masked vision and language modeling and 2) multi-modal alignment. We explain the details of each pre-training objective in this section.

### 3.1 Masked Vision and Language Modeling

The overall framework of masked vision and language modeling is shown in Figure 2. We use transformer-based encoders [49] for both image and text streams. Given an image-text pair  $(I, T)$ , an image encoder,  $f_{im}$ , is used to extract features,  $\mathbf{v} = \{v_{cls}, v_1, \dots, v_N\}$ , from the image input  $I$ .  $N$  is the number of image patches and  $v_{cls}$  is the encoding of the image class token, [CLS]. The text encoder,  $f_{txt}$ , extracts features,  $\mathbf{w} = \{w_{cls}, w_1, \dots, w_M\}$ , from the text input,  $T$ .  $M$  is the number of text tokens and  $w_{cls}$  is the encoding of the start token of a sentence, [START]. The image and the text encoder consist of 12 self-attention blocks as shown in Figure 3 (a). The image and the text features are further processed by image and text cross-modality encoders. The cross-modality encoders have 3 cross-attention blocks as illustrated in Figure 3 (b). The image (text) cross-modality encoder uses text (image) features to generate attentions. These cross-modality encoders can enhance the representation of one modality by interacting with another modality [32, 47].

**Image and Text Masking:** For text masking, we follow BERT [10] with minor modifications. In BERT, the original tokens are replaced with either the [MASK] token or random tokens. We use only the [MASK] token to replace tokens to be masked [50]. For image masking, we follow [17, 52] and use random masking of raw image patches with a masking patch size of  $32 \times 32$ . Given that  $224 \times 224$  images are divided into  $16 \times 16$  patches for the image encoder, the large masking patch prevents the model from simply copying their neighborhood pixels for reconstruction [52].

**Joint Reconstruction:** We reconstruct the original signals of one modality from its masked input conditioned on the unmasked input of the other modality. Specifically, an original image,  $I$ , and a masked text,  $T_m$ , are used to reconstruct an original text,  $T$ , and similarly a masked image,  $I_m$ , and an original text,  $T$ , are used to reconstruct the original image,  $I$ . For image reconstruction,  $(I_m, T)$  is first given to the image and the text encoders to obtain masked image features,  $\mathbf{v}_m$ , and unmasked text features,  $\mathbf{w}$ . Following [52], we use both masked and unmasked patches to obtain  $\mathbf{v}_m$ .  $(\mathbf{v}_m, \mathbf{w})$  are further processed by the image cross-modality encoder,  $g_{im}$ , where  $\mathbf{w}$  is used to compute cross-attentions. The output of  $g_{im}$  is mapped back to the original RGB image space by an image cross-modality decoder,  $g_{im}^{de}$ , which consist of 3 cross-attention blocks followed by a fully connected layer (FC). Although existing work exploits a light-weight transformer decoder with only self-attention [17] or a simple linear mapping [52] for the image decoder, we use joint information between modalities in decoding. For masked text reconstruction, a token classifier,  $g_{txt}^{de}$ , which consists of a FC followed by softmax is applied to the output of the text cross-modality encoder,  $g_{txt}$ , for the token prediction. The masked V+L modeling loss,  $\mathcal{L}_{MVLM}$ , is defined as

$$\mathcal{L}_{MVLM} = \underbrace{\mathcal{H}(y_T, \phi_{txt}(I, T_m))}_{\text{MLM}} + \underbrace{\mathbb{E}_{(I,T) \sim D} \left[ \frac{1}{\Omega(I^M)} \|\mathbf{I}^M - \phi_{im}^M(I_m, T)\|_1 \right]}_{\text{MIM}}, \quad (1)$$

where  $\phi_{txt} = g_{txt}^{de}(g_{txt}(f_{im}(I), f_{txt}(T_m)))$  and  $\phi_{im} = g_{im}^{de}(g_{im}(f_{im}(I_m), f_{txt}(T)))$ . A pair of  $I$  and  $T$  are sampled from the training dataset  $D$ ,  $\mathcal{H}$  denotes cross-entropy, and  $y_T$  is a matrix that contains one-hot row vectors for the ground truth tokens of the text,  $T$ . MIM loss is computed only for masked pixels. Hence, the superscript  $M$  on  $I$  and  $\phi_{im}$  denotes the set of the masked pixels.  $\Omega(\cdot)$  is the number of pixels. When minimizing  $\mathcal{L}_{MVLM}$ , the model is enforced to reconstruct the original signals by attending to the other modality signals. Cross-attending for reconstruction enables the model to learn interaction between V+L modalities.

### 3.2 Multi-modal Alignment

In addition to the masked signal modeling tasks, we adopt two additional tasks to explicitly learn multi-modality alignment. The first one is an image-text contrastive (ITC) learning [37, 19]. For the  $k$ -th pair of image and text features out of the image and text encoders, two separate FC layers are used to project the image [CLS] token features and the text [START] token features to the same dimensional feature space with unit norm,  $z_{im}^k$  and  $z_{txt}^k$ , respectively. The loss,  $\mathcal{L}_{ITC}$  is computed as

$$\mathcal{L}_{ITC} = -\frac{1}{N} \sum_{k=1}^N \left[ \log \frac{\exp(z_{im}^k \cdot z_{txt}^k / \tau)}{\sum_{n=1}^N \exp(z_{im}^k \cdot z_{txt}^n / \tau)} + \log \frac{\exp(z_{im}^k \cdot z_{txt}^k / \tau)}{\sum_{n=1}^N \exp(z_{im}^n \cdot z_{txt}^k / \tau)} \right], \quad (2)$$

where  $N$  and  $\tau$  are the batch size and the temperature scaling parameter, respectively. The second task is an image-text matching (ITM) [6, 26, 28], predicting whether an image and a text are aligned

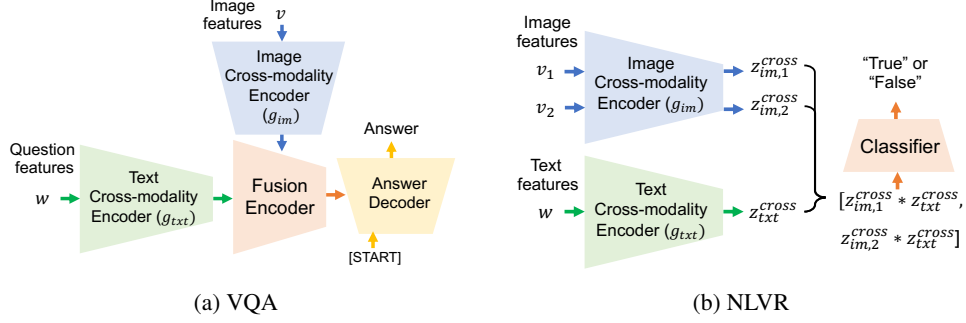


Figure 4: An illustration of model architectures for VQA and NLVR.

or not. The [CLS] and [START] token features from the image and text cross-modality encoders are  $z_{im}^{cross}$  and  $z_{txt}^{cross}$ , respectively. To fuse these two features, we compute the element-wise product of  $z_{im}^{cross}$  and  $z_{txt}^{cross}$  ( $z_{im}^{cross} * z_{txt}^{cross}$ ), and a FC layer followed by softmax is applied to obtain the final prediction. For training, we use  $y_{ITM} = 1$ , when  $z_{im}^{cross}$  and  $z_{txt}^{cross}$  are a pair. Otherwise,  $y_{ITM} = 0$ . The loss,  $\mathcal{L}_{ITM}$ , is defined as

$$\mathcal{L}_{ITM} = \mathcal{H}(y_{ITM}, g^{itm}(z_{im}^{cross} * z_{txt}^{cross})). \quad (3)$$

Following [26], we sample in-batch hard negatives based on the distribution of the cosine similarity between  $z_{im}$  and  $z_{txt}$ . The overall pre-training loss,  $\mathcal{L}$ , is defined as  $\mathcal{L} = \mathcal{L}_{MVLM} + \mathcal{L}_{ITC} + \mathcal{L}_{ITM}$ . We term our model trained with loss  $\mathcal{L}$  as MaskVLM (**M**asked **V**ision and **L**anguage **M**odeling).

### 3.3 Probabilistic interpretation

We differentiate MaskVLM from the existing V+L models using masked signal modeling from a perspective of likelihood estimation. The training objective of masked signal modeling on uni-modal signals,  $X$ , focuses on learning the data distribution  $p(X)$  which is formulated by the law of total probability as  $p(X) = \sum_{X_m \in \mathcal{M}_X} p(X_m) \cdot p(X|X_m)$ , where  $X_m$  is an instance of masked signal from the set of all possible masked signals,  $\mathcal{M}_X$ . MIM or MLM learns the data distribution by maximizing  $\sum_{X_m \in \mathcal{M}_X} p(X|X_m)$  [3].

In V+L representation learning, the ultimate goal is to learn the joint distribution of multi-modal signals,  $p(I, T)$ . However, the authors in [44] pointed out that directly maximizing the likelihood for the joint distribution is challenging because of the heterogeneous multi-modal data distributions. Instead, they show minimizing variation of information defined as  $-\mathbb{E}_{(I, T) \sim D}(\log p(I|T) + \log p(T|I))$  is sufficient to estimate the joint distribution. From a perspective of variation of information, the limitations in existing works can be better understood. Several existing works attempted to approximate the joint distribution using MLM with unmasked image [13, 26, 27, 53]. In other words,  $p(T|I, T_m)$  is maximized to learn the conditional distribution,  $p(T|I)$ , but  $p(I|T)$  is not modeled. In other existing works [6, 24, 32, 45, 47], where both modalities are masked, the visual masking is limited to mask the visual features extracted from a frozen object detector,  $\psi(\cdot)$ , instead of the raw image pixels. In this case, the distributions  $p(\psi(I)|T)$  and  $p(T|\psi(I))$  are modeled instead of  $p(I|T)$  and  $p(T|I)$ . This frozen feature extractor can bottleneck the direct estimation of the underlying data distribution. MaskVLM is trained end-to-end to estimate both conditional distributions,  $p(I|T)$  and  $p(T|I)$ , which directly minimizes the variation of information. We hypothesize this modeling of conditional distributions for both modalities could lead to superior performance in both large-scale and limited data training scenarios, which we empirically demonstrated in Section 4.

## 4 Experiments

### 4.1 Pre-training datasets and downstream tasks

We use the union of four datasets for pre-training so that we can perform a fair comparison with existing state-of-the-art methods [6, 26]. These datasets are Conceptual Captions (CC) [42], SBU Captions [34], Visual Genome (VG) [23], and COCO Captions [29]. While VG and COCO contain captions annotated by humans, CC and SBU captions are automatically collected from the web.



The total number of unique images and image-text pairs in the four datasets are 4.1M and 5.2M, respectively. We term this pre-training dataset as the 4M dataset. We validate the pre-trained model on the following four downstream tasks:

**Image-Text Retrieval:** We perform text-to-image and image-to-text retrieval. We use the ITC and ITM losses of Section 3.2 for finetuning and the finetuned models are evaluated on COCO [29] and Flickr30k [35]. In addition, since COCO is used for pre-training, zero-shot retrieval performance is reported on Flickr30k. In [26], the model finetuned on COCO is used for the zero-shot evaluation on Flickr30k. Although it may result in better performance, we believe that using finetuned models does not validate the zero-shot capability of the pre-trained model. Therefore, we use the pre-trained model directly for zero-shot evaluation. Following [26], we first retrieve top- $k$  candidates using the similarity scores from the image and the text encoders. The top- $k$  candidates are re-ranked by cross-modality encoders to obtain the final retrieval results.

**Visual Question Answering (VQA):** Here, given an image and a question pair, the model should generate a correct answer. The model is evaluated on VQA v2 [16]. We adopt the answer generation framework [7] and finetune the base model with a fusion encoder and an answer decoder as shown in Figure 4 (a). The fusion encoder consists of one cross-attention block shown in Figure 3 (b). The output from the text cross-modality encoder is used as queries, and the image cross-modality encoder output is utilized to create attentions in the fusion encoder. The architecture of the answer decoder is the same as that of the text cross-modality encoder, but it is trained with a language modeling loss to generate the answers. Specifically, the output of the fusion encoder is used for computing attentions and the answer tokens are autoregressively predicted. During inference, [START] token is used as an initial token to generate following answer tokens. The fusion encoder and the answer decoder are initialized by the last and all three blocks of the pre-trained text cross-modality encoder, respectively.

**Natural Language for Visual Reasoning (NLVR):** This task involves a binary classification with a triplet, (text, image1, image2). The goal here is to predict whether the text describes the pair of images. For finetuning, we feedforward (text, image1) and (text, image2) separately to extract the features as shown in Figure 4 (b). The [CLS] token features of image1 and image2 from the image encoder are denoted as  $v_1$  and  $v_2$ , respectively. The [START] token text features from the text encoder is  $w$ . These features are processed by the cross-modality encoders. The outputs of the image and text cross-modality encoders are fused by element-wise multiplication. The fused features for both images are concatenated, and a classifier with two linear layers predicts whether the text is aligned with the image pair or not. Different from [13, 26, 53], where the models require additional text-assignment pre-training step before finetuning, we directly finetune for simplicity. NLVR2 [46] is used for the evaluation.

**Visual Entailment (VE):** Given an image text pair, the task is to classify the relationship between the image and the text into one of three categories: entailment, neutral, and contradictory. The element-wise product of the output from the image and the text cross-modality encoders is forwarded to a classifier of two linear layers for prediction. SNLI-VE [51] is used for evaluation.

## 4.2 Implementation details

We use a Visual Transformer (ViT) [11] pre-trained on ImageNet [9] and a pre-trained RoBERTa from [30] to initialize the image and the text encoder, respectively. We pre-train the model for 50 epochs when the 4M dataset is used and 30 epochs for all other experiments. A batch size of 512 is used with 16 NVIDIA Tesla V100 GPUs. All parameters are optimized using AdamW [31] with a weight decay of 0.05. Following [52], we use the image masking ratio of 60%. While 15% masking ratio is used for text in language models [10, 30], we use 30% since the paired image can provide additional information for text reconstruction. During pre-training, the learning rate is warmed up to  $3 \times 10^{-4}$  in the first 5 epochs and decayed to  $3 \times 10^{-5}$  using a cosine scheduler. The learning rates for the image encoder and the text encoder are set to  $10^{-5}$ , which is less than that of the cross-modality encoders. An image size of  $224 \times 224$  and RandAugment [8] are used. During finetuning, the image is resized to  $384 \times 384$  and the positional encoding is interpolated following [11]. More details on finetuning for each downstream task can be found in supplementary materials.

## 4.3 Evaluation on Image-Text Retrieval, VQA, NLVR, and VE

We compare the finetuned image-text retrieval performance of the proposed MaskVLM with the state-of-the-art methods in Table 1. The second column is the number of unique images used for

Method	# images	MSCOCO (5K)						Flickr30k (1K)					
		Image Retrieval			Text Retrieval			Image Retrieval			Text Retrieval		
		R@1	R@5	R@10	R@1	R@5	R@10	R@1	R@5	R@10	R@1	R@5	R@10
ImageBERT [36]	6M	50.5	78.7	87.1	66.4	89.8	94.4	73.1	92.6	96.0	87.0	97.6	99.2
UNITER [6]	4M	52.9	79.9	88.0	65.7	88.6	93.8	75.6	94.1	96.8	87.3	98.0	99.8
VILLA [15]	4M	-	-	-	-	-	-	76.3	94.2	96.8	87.9	97.5	98.8
OSCAR [28]	4M	54.0	80.8	88.5	70.0	91.1	95.5	-	-	-	-	-	-
ALBEF [26]	4M	56.8	81.5	89.2	73.1	91.4	96.0	82.8	<b>96.7</b>	<b>98.4</b>	94.3	<b>99.4</b>	99.8
Triple [53]	4M	59.0	83.2	89.9	75.6	92.8	96.7	84.0	<b>96.7</b>	<b>98.5</b>	94.9	<b>99.5</b>	99.8
Codebook [13]	4M	58.7	82.8	89.7	75.3	92.6	96.6	83.3	96.1	97.8	95.1	<b>99.4</b>	<b>99.9</b>
ALIGN [19]	1.2B	59.9	83.3	89.8	77.0	93.5	96.9	84.9	97.4	98.6	95.3	99.8	100.0
MaskVLM	4M	<b>60.1</b>	<b>83.6</b>	<b>90.4</b>	<b>76.3</b>	<b>93.8</b>	<b>96.8</b>	<b>84.5</b>	<b>96.7</b>	<b>98.2</b>	<b>95.6</b>	<b>99.4</b>	<b>99.9</b>

Table 1: Comparison with finetuned state-of-the-art methods on image-text retrieval. The gray row indicates that the model is trained with significantly larger number of data than MaskVLM.

Method	# images	Flickr30k (1K)					
		Image Retrieval			Text Retrieval		
		R@1	R@5	R@10	R@1	R@5	R@10
ImageBERT [36]	6M	54.3	79.6	87.5	70.7	90.2	94.0
Unicoder-VL [24]	3.8M	48.4	76.0	85.2	64.3	85.8	92.3
ViLT [22]	4M	55.0	82.5	89.8	73.2	93.6	96.5
UNITER [6]	4M	66.2	88.4	92.9	80.7	95.7	98.0
ALBEF [26]	4M	68.2	88.6	93.0	84.9	97.2	99.0
CLIP [37]	400M	68.7	90.6	95.2	88.0	98.7	99.4
ALIGN [19]	1.2B	75.7	93.8	96.8	88.6	98.7	99.7
MaskVLM	4M	<b>75.0</b>	<b>92.5</b>	<b>95.8</b>	<b>87.0</b>	<b>97.9</b>	<b>99.3</b>

Table 2: Zero-shot image-text retrieval performance on Flickr30k. The gray row indicates that the model is trained with significantly larger number of data than MaskVLM

pre-training and the retrieval performance is evaluated in terms of Recall@k (R@k). We do not directly compare with ALIGN [19] since it is trained with 300 times more data than MaskVLM. However, we still highlight the small performance gap between MaskVLM and ALIGN, which is obtained with extremely less amount of data. We achieve the best performance in all Recall@k metrics on both COCO and Flickr30k except for the image retrieval R@10 and text retrieval R@5 on Flickr30k. Compared to ALIGN, we even achieve higher R@1 for image retrieval on COCO and text retrieval on Flickr30k. We close the gap as small as 0.7 and 0.4 at R@1 of text retrieval on COCO and image retrieval on Flickr30k, respectively. Table 2 shows the zero-shot retrieval performance of the state-of-the-art methods on Flickr30k. MaskVLM achieves a significant improvement over the second best method, ALBEF [26], by 6.8 point at R@1 for image retrieval. Given that ALBEF is trained with MLM only, we hypothesize that the significant improvement in image retrieval is obtained by additional MIM in MaskVLM, which models  $p(I|T)$ . Compared with CLIP [37] which is trained with at least 100 times more data than MaskVLM, we still achieve higher R@1 for image retrieval by 6.3 point. In general, MaskVLM achieves state-of-the-art performance in both finetuning and zero-shot experiments.

We report the accuracies on VQA, NLVR, and VE in Table 3. VQA, NLVR, and VE models require additional heads on top of the pre-trained model and are finetuned with different loss functions which are not used during pre-training. Hence, evaluation on these tasks shows the generalizability of the V+L model across a broad range of V+L tasks. We consistently achieve the best performances in all these tasks except for the validation split of NLVR2. In particular, MaskVLM is better than the second best method by 0.43, 1.14, and 0.27 on the test splits of VQA, NLVR2, and SNLI-VE, respectively.

#### 4.4 Evaluation with limited pre-training data

We highlight the performance of MaskVLM in limited data scenarios. In particular, we create three subsets of the 4M pre-training data by sampling 50%, 25%, and 10% of CC and combining them with COCO. The number of image-text pairs in each subset is around 39%, 25%, and 16% of the

Method	VQA		NLVR2		SNLI-VE	
	test-dev	test-std	dev	test-P	val	test
VisualBERT [27]	70.80	71.00	67.40	67.00	-	-
VL-BERT [45]	71.16	-	-	-	-	-
LXMERT [47]	72.42	72.54	74.90	74.50	-	-
12-in-1 [32]	73.15	-	-	78.87	-	76.95
UNITER [6]	72.70	72.91	77.18	77.85	78.59	78.28
VL-BART/T5 [7]	-	71.30	-	73.60	-	-
ViLT [22]	70.94	-	75.24	76.21	-	-
OSCAR [28]	73.16	73.44	78.07	78.36	-	-
VILLA [15]	73.59	73.67	78.39	79.30	79.47	79.03
ALBEF [26]	74.54	74.70	80.24	80.50	80.14	80.30
Triple [53]	74.90	74.92	80.54	80.11	<b>80.51</b>	80.29
Codebook [13]	74.86	74.97	80.50	80.84	<b>80.47</b>	80.40
MaskVLM	<b>75.45</b>	<b>75.40</b>	<b>81.58</b>	<b>81.98</b>	<b>80.37</b>	<b>80.67</b>

Table 3: Comparison with state-of-the-art methods on VQA, NLVR2, and VE.

Dataset (# of samples)	Method	Image Retrieval		Text Retrieval	
		R@1	R@5	R@1	R@5
CC 50% + COCO (2M)	ALBEF	49.97	77.35	65.76	89.32
	Codebook	53.21	79.74	69.42	90.5
	MaskVLM	<b>56.36</b>	<b>81.98</b>	<b>73.22</b>	<b>92.00</b>
CC 25% + COCO (1.3M)	ALBEF	48.09	75.63	64.24	87.20
	Codebook	52.22	79.18	68.80	89.90
	MaskVLM	<b>55.11</b>	<b>81.28</b>	<b>72.18</b>	<b>91.48</b>
CC 10% + COCO (0.9M)	ALBEF	45.33	73.57	61.00	84.98
	Codebook	50.80	78.26	66.96	89.62
	MaskVLM	<b>54.04</b>	<b>80.74</b>	<b>70.04</b>	<b>91.24</b>

Table 4: Image-text retrieval performance on COCO with limited pre-training data.

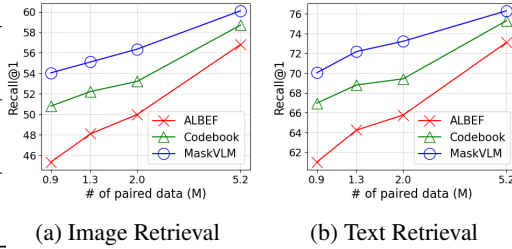


Figure 5: R@1 plots for image and text retrieval on COCO using limited pre-training data.

4M pre-training data which contain 5.2M pairs, respectively. We pre-train models with these subsets of the data and analyze the image-text retrieval performance in comparison with state-of-the-art methods. The results on COCO are reported in Table 4 and also R@1 performance is visualized in Figure 5. We particularly compare MaskVLM with the most recent state-of-the-art methods, which are ALBEF [26] and Codebook [13]. When the model is pre-trained with the 4M dataset, the R@1 gaps between ALBEF and MaskVLM are 3.3 and 3.2 for image and text retrieval, respectively. However, when limited data is used for pre-training, the image and the text retrieval R@1 gaps drastically increase to 6.39 and 7.46 in CC 50% + COCO and 8.71 and 9.04 in CC 10% + COCO, respectively. While Codebook shows competitive recall performance compared to the MaskVLM, the R@1 differences in image and text retrieval, respectively, increase from 1.4 and 1.0 in 4M dataset to 3.15 and 3.80 in CC 50% + COCO. Our model trained with CC25% + COCO outperforms Codebook trained with CC50% + COCO by 1.90 and 2.76 points in terms of image and text retrieval R@1, respectively. Similar to ALBEF, Codebook also relies only on MLM and does not model masked images. Since the main difference between MaskVLM and these methods is the additional MIM in MaskVLM, we believe that joint modeling of V+L contribute to better performance in limited data scenarios.

#### 4.5 Ablation study

We perform an ablation study using different combinations of loss components to highlight the contribution of masked V+L modeling. We compare four models with the same architecture but with different loss functions for pre-training: *i*) ITC + ITM, *ii*) ITC + ITM + MLM, *iii*) ITC + ITM + MIM, and *iv*) ITC + ITM + MLM + MIM, where MLM and MIM are defined in (1). We pre-train all models on CC 50% + COCO dataset and compare finetuning and zero-shot retrieval performance on Flickr30k in Table 5. In finetuning performance, additional MLM loss on top of ITC +ITM slightly improves image retrieval R@1 by 0.38 and achieves comparable performance in text retrieval (*i* vs. *ii*). On the other hand, when MLM + MIM is used with ITC + ITM, the model achieves significant improvement over ITC + ITM + MLM by 0.92 and 2.10 for R@1 image and text retrieval, respectively. ITC + ITM + MLM + MIM also obtains the best performance in zero-shot retrieval.



Loss	Finetuned				Zero-shot			
	IR		TR		IR		TR	
	R@1	R@5	R@1	R@5	R@1	R@5	R@1	R@5
ITC + ITM	79.96	95.56	92.30	98.90	69.50	89.54	82.40	96.60
ITC + ITM + MLM	80.34	95.82	92.00	99.30	70.74	90.92	84.40	97.10
ITC + ITM + MIM	80.12	95.56	91.56	99.00	69.26	90.30	82.90	97.20
ITC + ITM + MLM + MIM	<b>81.26</b>	<b>96.00</b>	<b>94.10</b>	<b>99.60</b>	<b>71.18</b>	<b>91.12</b>	<b>85.60</b>	<b>97.50</b>

Table 5: Image-text retrieval evaluation on Flickr30k with different loss functions for pre-training.

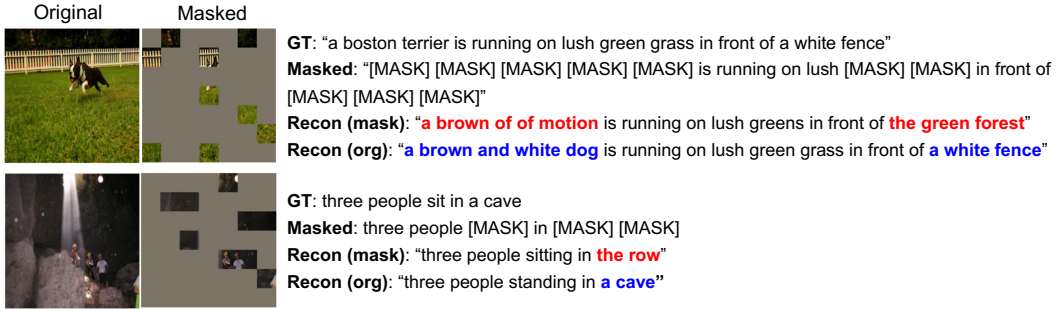


Figure 6: Masked language modeling examples using masked and original images. "Recon (mask)" and "Recon (org)" denote reconstructed text from the masked image and the original image, respectively.

This result further supports our probabilistic interpretation and the advantage of joint modeling for masked V+L signals.

#### 4.6 Qualitative results

We perform a qualitative analysis to show the role of multi-modal information in the reconstruction of masked signals from our model. To be specific, we illustrate the prediction of masked text tokens with and without the corresponding images. This illustration highlights how MaskVLM effectively utilizes both modality information to complete the masked signal modeling task. Figure 6 shows the reconstruction of masked texts using original images ("Recon (org)") and masked images ("Recon (mask)"). In the first top example, when the model is given a masked text and a masked image which does not contain the "dog", the reconstruction is performed by using only available information such as image patches of "green grass". Thus, the prediction is limited to "a brown of motion" or "the green forest". However, when original image is used for reconstruction, both "a brown and white dog" and "white fence" are reconstructed by accurately attending to the image. In the bottom example, the visible patches of the masked image contain a few people, but lack background information. Consequently, the reconstruction with the masked image does not contain any background information but the background "cave" is reflected in the reconstruction with the original image. These examples confirm that MaskVLM has learned to perform masked signal modeling using both V+L information.

## 5 Conclusion

We propose masked vision and language modeling as a pre-training task for learning V+L representations. We provide a probabilistic interpretation to highlight the contribution of the proposed method and validate its advantages in both large-scale and limited data regimes. We consistently achieve the state-of-the-art performance in a broad range of V+L tasks.

**Limitations and potential negative social impacts:** We investigate the effectiveness of the proposed method in the scale of a few millions of image-text pair data or less. Although the proposed method achieves powerful performance in limited data regimes, its capability with significantly larger amount of data (hundreds of millions or more) as discussed in CLIP [37] has not been explored yet and remains as a future work. We note that since the model is trained with data automatically collected from web, proper filtering of the pre-training data is required before the deployment of the model to prevent the model from being biased toward certain races, genders, ages etc.

## References

- [1] Tarik Arici, Mehmet Saygin Seyfioglu, Tal Neiman, Yi Xu, Son Train, Trishul Chilimbi, Belinda Zeng, and Ismail Tutar. Mlim: Vision-and-language model pre-training with masked language and image modeling. *arXiv preprint arXiv:2109.12178*, 2021. 3
- [2] Hangbo Bao, Li Dong, and Furu Wei. Beit: Bert pre-training of image transformers. *arXiv preprint arXiv:2106.08254*, 2021. 1, 3
- [3] Yoshua Bengio, Li Yao, Guillaume Alain, and Pascal Vincent. Generalized denoising auto-encoders as generative models. *Advances in neural information processing systems*, 26, 2013. 5
- [4] Zhaowei Cai, Gukyeong Kwon, Avinash Ravichandran, Erhan Bas, Zhuowen Tu, Rahul Bhotika, and Stefano Soatto. X-detr: A versatile architecture for instance-wise vision-language tasks. *arXiv preprint arXiv:2204.05626*, 2022. 1
- [5] Mark Chen, Alec Radford, Rewon Child, Jeffrey Wu, Heewoo Jun, David Luan, and Ilya Sutskever. Generative pretraining from pixels. In *International Conference on Machine Learning*, pages 1691–1703. PMLR, 2020. 3
- [6] Yen-Chun Chen, Linjie Li, Licheng Yu, Ahmed El Kholy, Faisal Ahmed, Zhe Gan, Yu Cheng, and Jingjing Liu. Uniter: Universal image-text representation learning. In *European conference on computer vision*, pages 104–120. Springer, 2020. 2, 3, 4, 5, 7, 8, 13
- [7] Jaemin Cho, Jie Lei, Hao Tan, and Mohit Bansal. Unifying vision-and-language tasks via text generation. In *International Conference on Machine Learning*, pages 1931–1942. PMLR, 2021. 6, 8
- [8] Ekin D Cubuk, Barret Zoph, Jonathon Shlens, and Quoc V Le. Randaugment: Practical automated data augmentation with a reduced search space. In *Proceedings of the IEEE/CVF Conference on Computer Vision and Pattern Recognition Workshops*, pages 702–703, 2020. 6, 13
- [9] Jia Deng, Wei Dong, Richard Socher, Li-Jia Li, Kai Li, and Li Fei-Fei. Imagenet: A large-scale hierarchical image database. In *2009 IEEE conference on computer vision and pattern recognition*, pages 248–255. Ieee, 2009. 6
- [10] Jacob Devlin, Ming-Wei Chang, Kenton Lee, and Kristina Toutanova. Bert: Pre-training of deep bidirectional transformers for language understanding. *arXiv preprint arXiv:1810.04805*, 2018. 1, 3, 4, 6
- [11] Alexey Dosovitskiy, Lucas Beyer, Alexander Kolesnikov, Dirk Weissenborn, Xiaohua Zhai, Thomas Unterthiner, Mostafa Dehghani, Matthias Minderer, Georg Heigold, Sylvain Gelly, et al. An image is worth 16x16 words: Transformers for image recognition at scale. *arXiv preprint arXiv:2010.11929*, 2020. 6, 13
- [12] Zi-Yi Dou, Yichong Xu, Zhe Gan, Jianfeng Wang, Shuohang Wang, Lijuan Wang, Chenguang Zhu, Pengchuan Zhang, Lu Yuan, Nanyun Peng, et al. An empirical study of training end-to-end vision-and-language transformers. In *Proceedings of the IEEE/CVF Conference on Computer Vision and Pattern Recognition*, pages 18166–18176, 2022. 3
- [13] Jiali Duan, Liqun Chen, Son Tran, Jinyu Yang, Yi Xu, Belinda Zeng, Chenyang Tao, and Trishul Chilimbi. Multi-modal alignment using representation codebook. *arXiv preprint arXiv:2203.00048*, 2022. 1, 3, 5, 6, 7, 8
- [14] Tsu-Jui Fu, Linjie Li, Zhe Gan, Kevin Lin, William Yang Wang, Lijuan Wang, and Zicheng Liu. Violet: End-to-end video-language transformers with masked visual-token modeling. *arXiv preprint arXiv:2111.12681*, 2021. 3
- [15] Zhe Gan, Yen-Chun Chen, Linjie Li, Chen Zhu, Yu Cheng, and Jingjing Liu. Large-scale adversarial training for vision-and-language representation learning. *Advances in Neural Information Processing Systems*, 33:6616–6628, 2020. 7, 8
- [16] Yash Goyal, Tejas Khot, Douglas Summers-Stay, Dhruv Batra, and Devi Parikh. Making the v in vqa matter: Elevating the role of image understanding in visual question answering. In *Proceedings of the IEEE conference on computer vision and pattern recognition*, pages 6904–6913, 2017. 6, 13
- [17] Kaiming He, Xinlei Chen, Saining Xie, Yanghao Li, Piotr Dollár, and Ross Girshick. Masked autoencoders are scalable vision learners. *arXiv preprint arXiv:2111.06377*, 2021. 1, 3, 4
- [18] Kaiming He, Haoqi Fan, Yuxin Wu, Saining Xie, and Ross Girshick. Momentum contrast for unsupervised visual representation learning. In *Proceedings of the IEEE/CVF conference on computer vision and pattern recognition*, pages 9729–9738, 2020. 1
- [19] Chao Jia, Yinfei Yang, Ye Xia, Yi-Ting Chen, Zarana Parekh, Hieu Pham, Quoc Le, Yun-Hsuan Sung, Zhen Li, and Tom Duerig. Scaling up visual and vision-language representation learning with noisy text supervision. In *International Conference on Machine Learning*, pages 4904–4916. PMLR, 2021. 1, 3, 4, 7

- [20] Aishwarya Kamath, Mannat Singh, Yann LeCun, Gabriel Synnaeve, Ishan Misra, and Nicolas Carion. Mdetr-modulated detection for end-to-end multi-modal understanding. In *Proceedings of the IEEE/CVF International Conference on Computer Vision*, pages 1780–1790, 2021. 1
- [21] Andrej Karpathy and Li Fei-Fei. Deep visual-semantic alignments for generating image descriptions. In *Proceedings of the IEEE conference on computer vision and pattern recognition*, pages 3128–3137, 2015. 13
- [22] Wonjae Kim, Bokyoung Son, and Ildoo Kim. Vilt: Vision-and-language transformer without convolution or region supervision. In *International Conference on Machine Learning*, pages 5583–5594. PMLR, 2021. 7, 8
- [23] Ranjay Krishna, Yuke Zhu, Oliver Groth, Justin Johnson, Kenji Hata, Joshua Kravitz, Stephanie Chen, Yannis Kalantidis, Li-Jia Li, David A Shamma, et al. Visual genome: Connecting language and vision using crowdsourced dense image annotations. *International journal of computer vision*, 123(1):32–73, 2017. 5, 13
- [24] Gen Li, Nan Duan, Yuejian Fang, Ming Gong, and Daxin Jiang. Unicoder-vl: A universal encoder for vision and language by cross-modal pre-training. In *Proceedings of the AAAI Conference on Artificial Intelligence*, pages 11336–11344, 2020. 2, 3, 5, 7
- [25] Junnan Li, Dongxu Li, Caiming Xiong, and Steven Hoi. Blip: Bootstrapping language-image pre-training for unified vision-language understanding and generation. *arXiv preprint arXiv:2201.12086*, 2022. 1, 3
- [26] Junnan Li, Ramprasaath Selvaraju, Akhilesh Gotmare, Shafiq Joty, Caiming Xiong, and Steven Chu Hong Hoi. Align before fuse: Vision and language representation learning with momentum distillation. *Advances in Neural Information Processing Systems*, 34, 2021. 1, 3, 4, 5, 6, 7, 8, 13
- [27] Liunian Harold Li, Mark Yatskar, Da Yin, Cho-Jui Hsieh, and Kai-Wei Chang. Visualbert: A simple and performant baseline for vision and language. *arXiv preprint arXiv:1908.03557*, 2019. 1, 2, 5, 8
- [28] Xiujun Li, Xi Yin, Chunyuan Li, Pengchuan Zhang, Xiaowei Hu, Lei Zhang, Lijuan Wang, Houdong Hu, Li Dong, Furu Wei, et al. Oscar: Object-semantics aligned pre-training for vision-language tasks. In *European Conference on Computer Vision*, pages 121–137. Springer, 2020. 2, 4, 7, 8
- [29] Tsung-Yi Lin, Michael Maire, Serge Belongie, James Hays, Pietro Perona, Deva Ramanan, Piotr Dollár, and C Lawrence Zitnick. Microsoft coco: Common objects in context. In *European conference on computer vision*, pages 740–755. Springer, 2014. 5, 6, 13
- [30] Yinhan Liu, Myle Ott, Naman Goyal, Jingfei Du, Mandar Joshi, Danqi Chen, Omer Levy, Mike Lewis, Luke Zettlemoyer, and Veselin Stoyanov. Roberta: A robustly optimized bert pretraining approach. *arXiv preprint arXiv:1907.11692*, 2019. 1, 3, 6
- [31] Ilya Loshchilov and Frank Hutter. Decoupled weight decay regularization. *arXiv preprint arXiv:1711.05101*, 2017. 6, 13
- [32] Jiasen Lu, Vedanuj Goswami, Marcus Rohrbach, Devi Parikh, and Stefan Lee. 12-in-1: Multi-task vision and language representation learning. In *Proceedings of the IEEE/CVF Conference on Computer Vision and Pattern Recognition*, pages 10437–10446, 2020. 2, 3, 4, 5, 8
- [33] Ron Mokady, Amir Hertz, and Amit H Bermano. Clipcap: Clip prefix for image captioning. *arXiv preprint arXiv:2111.09734*, 2021. 3
- [34] Vicente Ordonez, Girish Kulkarni, and Tamara Berg. Im2text: Describing images using 1 million captioned photographs. *Advances in neural information processing systems*, 24, 2011. 5
- [35] Bryan A Plummer, Liwei Wang, Chris M Cervantes, Juan C Caicedo, Julia Hockenmaier, and Svetlana Lazebnik. Flickr30k entities: Collecting region-to-phrase correspondences for richer image-to-sentence models. In *Proceedings of the IEEE international conference on computer vision*, pages 2641–2649, 2015. 6, 13
- [36] Di Qi, Lin Su, Jia Song, Edward Cui, Taroon Bharti, and Arun Sacheti. Imagebert: Cross-modal pre-training with large-scale weak-supervised image-text data. *arXiv preprint arXiv:2001.07966*, 2020. 7
- [37] Alec Radford, Jong Wook Kim, Chris Hallacy, Aditya Ramesh, Gabriel Goh, Sandhini Agarwal, Girish Sastry, Amanda Askell, Pamela Mishkin, Jack Clark, et al. Learning transferable visual models from natural language supervision. In *International Conference on Machine Learning*, pages 8748–8763. PMLR, 2021. 1, 3, 4, 7, 9
- [38] Alec Radford, Karthik Narasimhan, Tim Salimans, and Ilya Sutskever. Improving language understanding by generative pre-training. 2018. 3
- [39] Alec Radford, Jeffrey Wu, Rewon Child, David Luan, Dario Amodei, Ilya Sutskever, et al. Language models are unsupervised multitask learners. *OpenAI blog*, 1(8):9, 2019. 3
- [40] Aditya Ramesh, Prafulla Dhariwal, Alex Nichol, Casey Chu, and Mark Chen. Hierarchical text-conditional image generation with clip latents. *arXiv preprint arXiv:2204.06125*, 2022. 1

- [41] Aditya Ramesh, Mikhail Pavlov, Gabriel Goh, Scott Gray, Chelsea Voss, Alec Radford, Mark Chen, and Ilya Sutskever. Zero-shot text-to-image generation. In *International Conference on Machine Learning*, pages 8821–8831. PMLR, 2021. 1
- [42] Piyush Sharma, Nan Ding, Sebastian Goodman, and Radu Soricut. Conceptual captions: A cleaned, hypernymed, image alt-text dataset for automatic image captioning. In *Proceedings of the 56th Annual Meeting of the Association for Computational Linguistics (Volume 1: Long Papers)*, pages 2556–2565, 2018. 5
- [43] Sheng Shen, Liunian Harold Li, Hao Tan, Mohit Bansal, Anna Rohrbach, Kai-Wei Chang, Zhewei Yao, and Kurt Keutzer. How much can clip benefit vision-and-language tasks? *arXiv preprint arXiv:2107.06383*, 2021. 3
- [44] Kihyuk Sohn, Wenling Shang, and Honglak Lee. Improved multimodal deep learning with variation of information. *Advances in neural information processing systems*, 27, 2014. 5
- [45] Weijie Su, Xizhou Zhu, Yue Cao, Bin Li, Lewei Lu, Furu Wei, and Jifeng Dai. Vi-bert: Pre-training of generic visual-linguistic representations. *arXiv preprint arXiv:1908.08530*, 2019. 2, 3, 5, 8
- [46] Alane Suhr, Stephanie Zhou, Ally Zhang, Iris Zhang, Huajun Bai, and Yoav Artzi. A corpus for reasoning about natural language grounded in photographs. *arXiv preprint arXiv:1811.00491*, 2018. 6, 13
- [47] Hao Tan and Mohit Bansal. Lxmert: Learning cross-modality encoder representations from transformers. *arXiv preprint arXiv:1908.07490*, 2019. 2, 3, 4, 5, 8
- [48] Maria Tsimpoukelli, Jacob L Menick, Serkan Cabi, SM Eslami, Oriol Vinyals, and Felix Hill. Multimodal few-shot learning with frozen language models. *Advances in Neural Information Processing Systems*, 34:200–212, 2021. 1
- [49] Ashish Vaswani, Noam Shazeer, Niki Parmar, Jakob Uszkoreit, Llion Jones, Aidan N Gomez, Łukasz Kaiser, and Illia Polosukhin. Attention is all you need. *Advances in neural information processing systems*, 30, 2017. 4
- [50] Alexander Wettig, Tianyu Gao, Zexuan Zhong, and Danqi Chen. Should you mask 15% in masked language modeling? *arXiv preprint arXiv:2202.08005*, 2022. 4
- [51] Ning Xie, Farley Lai, Derek Doran, and Asim Kadav. Visual entailment: A novel task for fine-grained image understanding. *arXiv preprint arXiv:1901.06706*, 2019. 6, 13
- [52] Zhenda Xie, Zheng Zhang, Yue Cao, Yutong Lin, Jianmin Bao, Zhuliang Yao, Qi Dai, and Han Hu. Simmim: A simple framework for masked image modeling. *arXiv preprint arXiv:2111.09886*, 2021. 1, 3, 4, 6
- [53] Jinyu Yang, Jiali Duan, Son Tran, Yi Xu, Sampath Chanda, Liqun Chen, Belinda Zeng, Trishul Chilimbi, and Junzhou Huang. Vision-language pre-training with triple contrastive learning. *arXiv preprint arXiv:2202.10401*, 2022. 1, 3, 5, 6, 7, 8
- [54] Zhilin Yang, Zihang Dai, Yiming Yang, Jaime Carbonell, Russ R Salakhutdinov, and Quoc V Le. Xlnet: Generalized autoregressive pretraining for language understanding. *Advances in neural information processing systems*, 32, 2019. 1
- [55] Pengchuan Zhang, Xiujun Li, Xiaowei Hu, Jianwei Yang, Lei Zhang, Lijuan Wang, Yejin Choi, and Jianfeng Gao. Vinvl: Revisiting visual representations in vision-language models. In *Proceedings of the IEEE/CVF Conference on Computer Vision and Pattern Recognition*, pages 5579–5588, 2021. 2

## A Appendix

### A.1 Details on finetuning for downstream tasks

We explain implementation details for each of the downstream tasks. For all the downstream tasks, we use AdamW [31] with a weight decay of 0.05 and the cosine scheduler. An image size of  $384 \times 384$  with RandAugment [8] is utilized and the positional encoding is interpolated following [11]. Except for the VQA task, we use the model achieves the best performance in the validation set to report the performance on the test set. We use the last epoch model for the VQA evaluation.

**Image-Text Retrieval:** COCO [29] and Flickr30k [35] are used to report the performance. To be specific, we follow data splits proposed in [21] and an average recall over image and text retrieval is used to find the best model in the validation set. The pre-trained model is finetuned for 15 epochs with a batch size of 256 and a learning rate of  $1 \times 10^{-5}$ .

**Visual Question Answering (VQA):** For a fair comparison with existing methods [6, 26], we use training and validation sets from VQA v2.0 [16] with a subset of VQA samples from Visual Genome [23] for training. Also, we report performance on both test-dev and test-std splits of VQA v2.0. Following [26], we weight the loss for each answer based on its occurrence among all the answers. The model is finetuned for 15 epochs with a batch size of 256. We use a learning rate of  $2 \times 10^{-5}$  for the image and the text cross-modality encoders, the fusion encoder, and the answer decoder. For the image and the text encoders, a learning rate of  $1 \times 10^{-5}$  is used.

**Natural Language for Visual Reasoning (NLVR):** Data splits proposed in [46] are used for finetuning and evaluation. The model is finetuned for 5 epochs with a batch size of 128. Since the classifier is newly added after finetuning, we use a learning rate of  $1 \times 10^{-4}$  for the classifier and  $1 \times 10^{-5}$  for the remaining parts of the model.

**Visual Entailment (VE):** We follow data splits proposed in SNLI-VE [51]. We finetune the model with a batch size of 256 for 5 epochs. Similar to the NLVR task, a learning rate of  $1 \times 10^{-4}$  is used for the classifier and  $1 \times 10^{-5}$  is used for the remaining parts of the model.

### A.2 Evaluation on VQA, NLVR, VE with limited pre-training data

The image-text retrieval performance of MaskVLM trained with limited data is highlighted in Table 4 of Section 4.4. In Table 6, we also compare the VQA, NLVR, and VE performance of MaskVLM and ALBEF [26] with limited pre-training data. In particular, we use the same three subsets of the 4M dataset, CC 50% + COCO, CC 25% + COCO, and CC 10% + COCO, described in Section 4.4 for pre-training. MaskVLM consistently outperforms ALBEF in all the limited data scenarios and the tasks. In particular, as the size of pre-training data becomes smaller from CC 50% + COCO to CC 10% + COCO, the performance gap between MaskVLM and ALBEF increases from 1.17 to 1.79 in VQA and 0.31 to 1.24 in the test set of SNLI-VE. In NLVR2 and VQA, MaskVLM trained with CC 10% + COCO achieves higher accuracy than ALBEF trained with CC50% + COCO, which contains more than twice of image-text pairs in CC 10% + COCO. Overall, MaskVLM achieves state-of-the-art performance in the regimes of limited training data on a broad range of V+L tasks.

Dataset (# of samples)	Method	VQA test-dev	NLVR2 dev	NLVR2 test-P	SNLI-VE val	SNLI-VE test
CC 50% + COCO (2M)	ALBEF	73.07	76.58	76.89	79.20	79.19
	MaskVLM	<b>74.24</b>	<b>79.81</b>	<b>79.47</b>	<b>79.69</b>	<b>79.50</b>
CC 25% + COCO (1.3M)	ALBEF	72.65	75.20	76.78	78.84	78.96
	MaskVLM	<b>74.17</b>	<b>79.13</b>	<b>78.94</b>	<b>79.35</b>	<b>79.76</b>
CC 10% + COCO (0.9M)	ALBEF	72.14	74.81	74.64	78.51	78.36
	MaskVLM	<b>73.93</b>	<b>78.62</b>	<b>77.19</b>	<b>79.11</b>	<b>79.60</b>

Table 6: VQA, NLVR, VE performance with limited pre-training data.



### A.3 Ablation study on masking ratio

We perform ablation study using different masking ratios for masked vision and language modeling. In particular, we pre-train MaskVLM with several combinations of image and text masking ratios on the CC 50% + COCO dataset and report the finetuned image-text retrieval performance on Flickr30k in Table 7. We also report an average of R@k for image and text retrieval. When only image masking ratio is changed in the first three rows of the table, the difference between the maximum and the minimum of the average recall is 0.26 for image retrieval and 0.10 for text retrieval. This shows that MaskVLM achieves stable performance across the tested image masking ratios. From comparison between the second row and the last row, we observe that increasing the text masking ratio from 0.15 to 0.3 leads to higher recall performance for both image and text retrieval.

Masking ratio (image / text)	Image Retrieval				Text Retrieval			
	R@1	R@5	R@10	Average	R@1	R@5	R@10	Average
0.5 / 0.3	81.32	96.04	97.92	91.76	93.30	99.70	100.00	97.67
0.6 / 0.3	81.26	96.00	97.78	91.68	94.10	99.60	99.60	97.77
0.7 / 0.3	81.82	96.00	98.00	91.94	93.60	99.50	99.90	97.67
0.6 / 0.15	80.30	95.66	97.82	91.26	92.50	99.10	99.60	97.07

Table 7: Finetuned image-text retrieval performance on Flickr30k with different masking ratios for masked vision and language modeling.

### A.4 Additional examples for the qualitative analysis

We present additional examples for the qualitative analysis of MaskVLM in Figure 7. Similar to Figure 6, masked text tokens are reconstructed with masked images (“Recon (mask)”) and original images (“Recon (org)”). We highlight that MaskVLM utilizes both V+L information to reconstruct the text which corresponds to the given image.

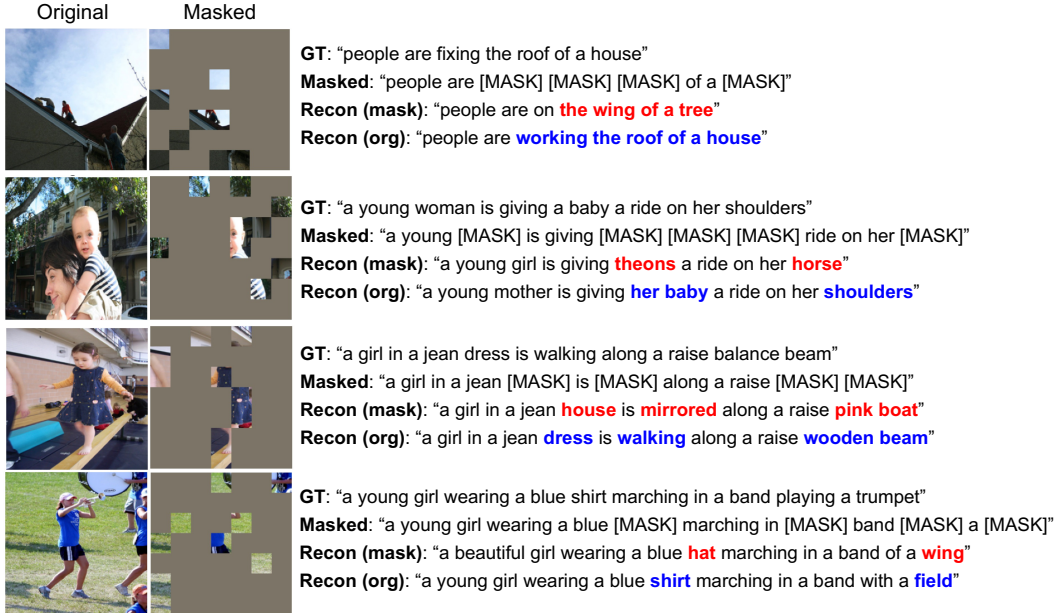


Figure 7: Additional masked language modeling examples using masked and original images. “Recon (mask)” and “Recon (org)” denote reconstructed text using the masked image and the original image, respectively.

### A.5 Statistics of the pre-training dataset

In Table 8, we report the statistics of the 4M pre-training dataset that MaskVLM is trained on. We note that some data urls provided in the web datasets can become invalid, which may lead to slightly different number of image-text pairs depending on when the datasets are downloaded.

Dataset	# of image-text pairs	# of images
COCO	566,747	113,287
CC	2,912,317	2,912,317
SBU	1,000,000	1,000,000
VG	768,536	100,406
<b>Total</b>	<b>5,247,600</b>	<b>4,126,010</b>

Table 8: Statistics of the 4M pre-training dataset.